Cellulose (2019) 26:3127–3141
https://doi.org/10.1007/s10570-019-02312-4

ORIGINAL RESEARCH

Preparation of nanofibrillated cellulose and nanocrystalline cellulose from surgical cotton and cellulose pulp in hot-glycerol medium

Anju Ramakrishnan · Kartik Ravishankar · Raghavachari Dhamodharan

Received: 9 October 2018 / Accepted: 1 February 2019 / Published online: 6 February 2019
© Springer Nature B.V. 2019

Abstract A simple and green method for the preparation of nanofibrillated cellulose (NFC) by heating surgical cotton in glycerol is demonstrated as an alternative to the existing mechanical degradation method. The heat treatment of cotton in the presence of 9% w/w sulphuric acid in glycerol (1 M), under relatively milder conditions than those reported in the literature in the absence of glycerol, resulted in the formation of nanocrystalline cellulose (NCC) due to extensive hydrolysis of the amorphous segments. The method reported offers certain unique advantages in the preparation of NFC such as high yield (71%) and much easier post-processing compared to the mechanical degradation method of preparation of NFC. It also offers certain unique advantages in the preparation of NCC such as relatively high yield (56%), the use of lesser quantity of sulphuric acid as well as elimination of the quenching of the reaction through the addition of excess water to the reaction mixture. The residual 'green solvent', separated by decantation or centrifugal separation, post-reaction, could be reused for several cycles after filtration with activated carbon. A simple utility of the NCC prepared as reinforcing additive to cement is demonstrated. The addition of 1% (w/w of cement) of NCC and tetraethylorthosilicate modified NCC enhanced the workability of cement mortar and the compressive strength of cured cement composite in sharp contrast to the use of microcrystalline cellulose that required 10% (w/w) for the same enhancement in strength but with poorer workability.

Graphical abstract A sustainable route for preparing NFC through heat treatment in glycerol is reported. In the presence of 1 M (9% w/w) sulphuric acid in glycerol, similar heat treatment resulted in the formation of both NFC and NCC. The residual 'green solvent' could be reused for several cycles. The addition of 1% (w/w) of nanocellulose prepared via this method enhanced the workability of cement mortar and the compressive strength of cured cement composite.

Raghavachari Dhamodharan: This work constitutes a part of Indian Patent Application No. 201841019186.

Electronic supplementary material The online version of this article (https://doi.org/10.1007/s10570-019-02312-4) contains supplementary material, which is available to authorized users.

A. Ramakrishnan · K. Ravishankar · R. Dhamodharan (✉)
Department of Chemistry, Indian Institute of Technology Madras, Chennai 600 036, India
e-mail: damo@iitm.ac.in

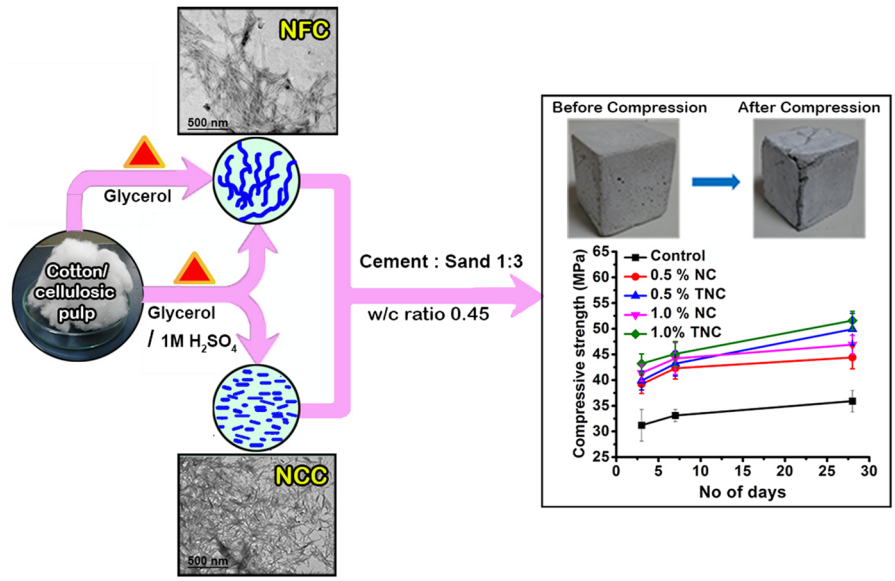

Keywords Agricultural biomass · Nanocellulose · Surface modification · Filler · Cement composite · Workability

Introduction

Biodegradable products from renewable resources such as cellulose, a major constituent of agricultural products and waste, with lesser detrimental effect on the environment and the health are in great demand. The main sources of cellulose are wood (soft/ hard), agricultural biomass and some animals (tunicates, some bacteria). Agriculture biomass wastes, which constitute abundant cellulose fiber, such as cotton stalk, corn stover, bagasse, pineapple/ palm leaf, rice/ wheat straw, flax, hemp, soy pods, rice husk, garlic straw, potato peel, grape skin, etc., are good sources of cellulose that are readily available and inexpensive.

Nanocellulose (NC), which is isolated from various cellulosic sources, has been gaining enormous attention due to its versatile applications in different fields of technology such as biomedical, personal hygiene products, nanocomposites, water purification, air filtering, food (gellant), food packaging, aerogel, gas barrier, biocatalyst (as nanocatalyst in the hydrolysis of esters) and flexible electronics (Chakraborty 2004; Islam et al. 2014; Kaushik and Moores 2016; Klemm et al. 2011; McCann et al. 1990; Sannino et al. 2009; Serizawa et al. 2013).

A range of nomenclature is being used to categorize the different forms of NC. It is therefore useful to follow a recent and relatively broad categorization (Kargarzadeh et al. 2017). Cellulose materials that are shorter in length (50–500 nm) and narrower in width (5–40 nm) and higher in crystallinity are referred as nanocrystalline cellulose (NCC) in this work (the literature defines them as NCC, CNC, CNW). These are highly stiff nano-rods extracted by eliminating the amorphous regions of cellulose fibers, conventionally, by strong mineral acid hydrolysis. Cellulose materials longer (upto 3000 nm), wider (< 100 nm), which are spaghetti like entangled nanofibers and generally obtained by the mechanical disintegration of the cellulosic biomasses, and lower in crystallinity are referred as nanofibrillated cellulose (NFC) (the literature defines them as NFC, CNF). The mechanical properties of nanocellulose (tensile strength ~ 500 MPa, stiffness of 140–220 GPa and a strength to weight ratio that is almost eight times that of stainless steel) enable it as a promising engineering material. It contains numerous hydroxyl groups on its surface that make it suitable for many chemical modifications, depending upon the end applications. The exponential increase in the number of publications and patents in this field clearly indicates the focus of researchers and industries towards large scale

production of nanocellulose (NC) (Rajinipriya et al. 2018).

Nanocellulose is prepared by a number of methods. The most common techniques used are: acid treatment (hydrolysis), enzymatic treatment, oxidation, electrospinning, high pressure and high temperature homogenization, high mechanical forces such as high shearing (with or without ultrasonic assistance), and steam explosion (Duran et al. 2012). Among the methods for the production of cellulose nanomaterials the most popular one is the chemical treatment involving strong mineral acid catalyzed hydrolysis initiated by the cleavage of the glycosidic bonds in the amorphous regions that link individual crystals. The optimized procedure involves treatment of cellulose biomass (after removal of lignin, hemi-cellulose and bleaching) with 64% (w/w) sulfuric acid at 45 °C for 1 h. In this process, sulfuric acid diffuses into the cellulose biomass and cleaves the glycosidic bonds and hydrolyses the amorphous cellulose and hemicelluloses at a much faster rate than the crystalline part of cellulose. During this process, the hydroxyl groups on the crystalline surface have been reported to undergo substitution by negatively charged sulfate groups, which could further impart electrostatic repulsion between NCC, giving additional stability for the dispersion. Since the non-crystalline region is removed during the acid hydrolysis, the degree of polymerization is expected to decrease and the crystallinity is expected to increase. The use of other mineral acids such as hydrochloric acid, hydrobromic acid and phosphoric acid for the preparation of NCC has also been reported in literature (Espinosa et al. 2013; Jia et al. 2013; Sadeghifar et al. 2011; Yu et al. 2013). It was reported that microwave irradiation or high intensity ultrasonication of microcrystalline cellulose (MCC) could shorten the reaction time of acid hydrolysis (Kos et al. 2014; Li et al. 2011). Organic dicarboxylic acids such as oxalic acid and maleic acid have also been used to hydrolyse cellulose at high temperature and pressure (Vom Stein et al. 2010). Nanocellulose has been isolated from hemp fibers using dodecyltrimethylammonium bromide followed by ultrasonication (Dai et al. 2013). The preparation of nanocellulose particles by using ionic liquid, 1-butyl-3-methylimidazolium hydrogen sulfate and investigation of the influence of reaction temperature (room temperature and at 90 °C) have also been reported (Xiao et al. 2015).

Despite the progress in nanocellulose research, many obstacles hamper its large-scale production and commercialization. The extraction of NFC is generally done through mechanical disintegration methods using ultrafine super friction grinder with a high pressure homogenizer for 8 to 16 h (Zimmermann et al. 2010). The process involves refining the pulp followed by high-pressure homogenization (various mechanical pretreatments such as grinding, milling, refining, cryocrushing, or ultrasonication are also required before homogenization). The refining process causes fibrillation by peeling the external cell wall layers and exposing the layer having the maximum quantity of cellulose upon which interfibrillar bonds break. This method is energy (of the order of 30 MWh/ton) intensive. Another technique to extract NFC is cryo-crushing, in which cellulose pulp is mechanically ground in a frozen state with a constant liquid nitrogen supply. The ice crystals, which are formed within the pulp, facilitate the breakage of the cell wall, to release nanofibrils of cellulose (Dufresne et al. 1997). The smaller fragments are later dispersed in water and loaded into high pressure homogenizer to obtain the NFC suspension. Some chemical pretreatments such as mild acid hydrolysis, enzymatic reactions, TEMPO mediated oxidation have been applied to the cellulosic pulp (Pääkko et al. 2007; Saito et al. 2007). This eases further mechanical treatment of microfibers and reduces a considerable amount of the energy consumption also (Dinand et al. 1999; Kamel 2007; Maiti et al. 2013). The cost-effectiveness and the environmental concern issues caused by the excess or expensive harsh chemical usage in the production of NCC retard its wide range application possibilities. It is evident from the literature that the concentrated acid facilitated hydrolysis is the preferred industrial method of choice for preparing NCC. It is fraught with the following two major difficulties: separation of sugars from the used sulphuric acid and recovery of the acid itself; gypsum is formed as a by-product when the excess acid is neutralized leading to another environmental problem to deal with. Dilute acid hydrolysis at high temperature results in the decomposition of glucose limiting the yield of nanocellulose.

The principle objective of this work was to explore the use of hot glycerol, a sustainable chemical, in the preparation of NFC and attempt to overcome some of the limitations associated with the production of NFC and NCC in large scale. The choice of glycerol arose

out of its sustainability, availability in abundance, high boiling point, solubility in water and the possibility to plasticize amorphous regions of cellulose enabling uniform heat transfer. Based on earlier literature reports on the low temperature pyrolysis of cellulose it was felt that heating the macrofibers of cellulose in glycerol may enable the defibrillation and depolymerisation/dehydration in the amorphous regions, due to uniform heat transfer, thereby leading to the formation of nanostructured cellulose under milder condition. Further it was expected that glycerol may facilitate the use of lower weight percentage of mineral acid facilitating the formation of NCC under milder conditions. These objectives are illustrated through the use of two distinct schemes for the isolation of nanocellulose from cotton. Due to its very high crystalline content with negligible amount of hemicelluloses/lignin (Maiti et al. 2013), no pre-treatment is required for cotton. The distinct schemes are: (1) 'green isolation' of NFC from cotton using thermal treatment with glycerol; (2) conversion of cotton into NCC by thermal treatment in minimum quantity of sulphuric acid in glycerol. In both the processes, the reaction solvent could be recovered back (by centrifugal separation) and reused for further cycles by a simple filtration using activated carbon. The yield, morphology and extent of crystallinity of purified samples were assessed. As one of the possible applications, the superior performances of NCC as well as surface modified NCC (with tetraethylorthosilicate) over microcrystalline cellulose (MCC) as cement admixture is demonstrated. The development of a simple and more environment-friendly (green) process that utilizes less harmful, water soluble, easily recoverable and recyclable chemicals, simplified purification and concentration/drying processes might address some of the limitations of large-scale production of NFC and NCC. Further, it may be noted that the method developed is also applicable to the bleached pulp (could be used without milling/grinding) obtained by pre-treatment of any cellulosic agricultural waste material.

Experimental section

Materials

The raw material, surgical cotton was supplied by R.K. Scientific limited, Chennai. All other chemicals, such as sodium hydroxide, hydrochloric acid, hydrogen peroxide, sulphuric acid and sodium hypochlorite, hydrogen peroxide, tetraethylorthosilicate (TEOS), liquid ammonia, glycerol, ethanol of analytical grade were purchased from RANKEM, Chennai and were used as received. River sand of particle size less than 2.36 mm and ordinary Portland cement confirming to 53 grade (IS 12269) were used for the preparation of cement mortar samples.

Isolation of nanofibrillated cellulose (NFC)

4.2 g of oven-dried cotton was added to 126 g of glycerol in a beaker. This was placed in an oil bath, maintained around 180–200 °C for a period of 4 h. After the reaction period, the mixture was removed from the oil bath and allowed to cool to room temperature, resulting in the formation of a white residue. The supernatant (glycerol) was decanted and reused. The residue was dispersed in water (40 ml) and centrifuged at 10,000 rpm for 10 min to remove any residual glycerol. The re-dispersion in water followed by centrifugation was done thrice. The residue (NFC) was either freeze-dried or dispersed in water to get an emulsion of NFC. The yield of NFC thus obtained from cotton was 71%.

Conversion of cotton into NCC

Oven-dried cotton fiber (1 g) was added to a mixture consisting of 9% w/w of sulphuric acid in glycerol such that the concentration was 1 M (cotton:solvent = 1:30 w/w). It was then heated in an oil bath maintained at 90 °C for a period of 3 h. The reaction mixture was then allowed to cool and centrifuged at 10,000 rpm for 10 min to remove the supernatant. The resulting residue was diluted with water (40 ml) and centrifuged at 10,000 rpm for 10 min. This procedure was repeated thrice to eliminate any residual solvent. NCC was collected as a turbid supernatant after mixing the above residue with water and centrifuging the suspension at a lower speed (6000 rpm for 10 min) for 5–6 times. The turbid supernatant was

concentrated by heating on a hot-plate. The final step of purification involved dialysis for 48 h to remove the residual acid/glycerol (required only if the pH of the dispersion of NCC was < 7) and then freeze-dried to isolate NCC. Yield of NCC: 56%; Transparent and flexible films of NCC were obtained by drying 5% NCC in water dispersion placed in a glass Petridish for 48 h at room temperature. It may be noted that the above conditions are optimal and process optimization details are not provided.

Surface modification of NCC with tetraethylorthosilicate (TEOS)

Tetraethylorthosilicate (TEOS) was used as the silane coupling agent for the surface modification of NCC into TNCC (Abdelmouleh et al. 2002).To a 1:4 ratio of water:ethanol medium (total volume 100 ml), 1 g of NCC and 20 mL of TEOS were added. Aqueous ammonia was added to this mixture until the pH was 11. Subsequently, the reaction vessel was placed in an oil bath provided with stirring and heated to 50 °C for 2 h.The wet sample was subjected to heat curing at 110 °C for 2 h. The product obtained was ground into a fine powder.

Preparation of cement mortar composite

The cement to sand ratio was taken as 1:3 (by weight). Various amounts of NCC and TEOS surface modified NCC (TNCC) (by weight of cement) were dispersed in the water required for the preparation of mortar. For compressive strength analysis, 50 mm cubes, with and without mineral admixtures, were cast using thoroughly fitted and oiled standard moulds (ASTM C109 2013). After 24 h, the mould was dismantled and the samples were set for water curing. The compressive strength of the samples was determined after 3, 7 and 28 days of curing time. Control experiments were done without adding any admixture by taking the water/cement ratio (w/c) as 0.4, 0.45 and 0.5, respectively.

Characterization

Powder X-ray diffraction patterns of all the materials were recorded with a Bruker D8 Advance diffractometer equipped with copper (Cu) anode (Cu Kα source of wavelength 1.5406 Å) at 40 kV and 30 mA in the region of 2θ from 5° to 80°. The crystallinity index of both raw material and nanocellulose was calculated and compared using the method reported (Park et al. 2010) as shown below.

$$CI\% = \frac{(I_{200} - I_{AM})}{I_{200}} \times 100 \quad (1)$$

In this equation, I_{200} represents the maximum intensity of the (200) plane reflection (at 2θ between 22° and 24°) and I_{AM} represents the intensity of the amorphous region (at 2θ of 18.3°), corresponding to the minimum intensity between the (110) and (200) planes (Segal et al. 1959). SEM images were obtained using Quanta 400 SEM with an acceleration voltage of 20 kV. The samples (dispersion in water), deposited on Si wafer, dried and were sputtered with gold, prior to the imaging. TEM images were taken using a Philips CM 12 TEM at an acceleration voltage of 120 kV. Image J software was used to measure the particle size distribution. The dispersions of 1% NFC and 1% NCC were deposited on carbon coated Cu grids under ambient conditions and dried for 2 h prior to use. Zetasizer Nano ZS90 analyser was used to measure zeta potential (by Laser Doppler microelectrophoresis) and the particle size distribution [using Dynamic Light Scattering (DLS)], at 25 °C, at 90° scattering angle. The water-based dispersions of 0.2% NFC and 0.2% NCC were used for zeta potential and DLS analyses. The thermogravimetric studies were carried out with TA Instruments Q500 Hi-Res TGA. All the samples (∼ 2 mg) were heated at 10 °C min^{-1} from room temperature to 600 °C, under nitrogen flow. Fourier transform infrared spectra (FT-IR) were acquired using JASCO 4100 FTIR spectrometer (JASCO, Japan). The solid samples required for the analysis were prepared in the pellet form by mixing 3–5 mg of the dry sample with 100 mg of dry potassium bromide (KBr). The transparency of NCC film was characterized by diffuse reflectance spectroscopy (DRS) using JASCO V-650 spectrophotometer. The workability of cement mortar (cement:sand ratio 1:3 by weight) with various amount of NCC and TNCC loading (0.5%, 1.0% and 1.5%weight of cement) was tested by flow table method (ASTM C1437)(ASTM C1437 2013). The compressive strength test of cement mortar specimens was determined by using Universal Testing Machine as per IS: 516-1959 after 3, 7, and 28 days of sample curing. The

value reported is the average of three different samples.

Results and discussion

The preparation of NCC from cotton linters, spruce wood, eucalyptus wood and Chinese silver grass by milling followed by glycolysis reaction in diol or glycerol, catalyzed by 3% methane sulphonic acid at 150 °C for 180 min was reported recently. The NCC prepared in this manner was finally rinsed with an organic solvent, dioxane (Kunaver et al. 2016).The processes reported here in the Schemes 1 and 2 are different from the recent work as we use either glycerol alone (for NFC isolation) or 1 M sulphuric acid in glycerol (for NCC isolation) without using another organic solvent. Further, no mechanical disintegration and homogenization operation is required in the process reported here. Further cotton or bleached pulp from cellulosic agricultural waste (the pre-treatment details for the preparation of bleached pulp are provided in the Supporting Information Figure S1) can also be used directly in the process. The photographs of different forms of NFC and NCC prepared from cotton are presented in Fig. 1.

The PXRD patterns of cotton, NFC and NCC are presented in Fig. 2. Surgical cotton shows the characteristic diffraction peaks of cellulose at $2\theta = 15.1°$, 16.5°, 22.9° and 35.1° which correspond to reflections from $[1\bar{1}0]$, [110], [200] and [004] crystallographic planes of cellulose I. The removal of significant portion of the amorphous regions in cotton is evident by the narrowing of the peaks in NFC and NCC. This is reflected quantitatively in the crystallinity index (CI) value, which increased from 79.2% for cotton to 92.8% for NFC. The change could be attributed to the effective plasticization action of glycerol that facilitates uniform heat transfer followed by depolymerisation/dehydration in the amorphous regions present in the cellulose precursors, which is reported for low temperature pyrolysis of cellulose as discussed later in the section on mechanism. It is well reported that acid treatment degrades cellulose-I more easily compared to cellulose-II (Lu et al. 2015), which could be considered as the reason for the further narrowing of diffraction peaks as observed in the case of NCC. This is also supported by the greater change in CI for NCC (97.9%) prepared by the acid catalyzed hot glycerol treatment. The higher CI values obtained may thus be due to more rapid hydrolysis of amorphous chains in cellulose, especially when catalyzed by the mineral acid. The corresponding PXRD patterns for NFC and NCC, isolated from bleached pulp are presented in the Supporting Information Figure S2. The crystallite size of cotton, NFC (cotton), NCC (cotton) samples perpendicular to (200) planes were also found out using Scherrer equation $L = K\lambda/\beta \cos\theta$, where θ is the diffraction angle, $\lambda = 0.154$ nm and β is angular full width at half maximum in radians of the (200) peak (Supporting information Table S1).

The TEM images of NFC and NCC obtained after hot-glycerol treatment of cotton are shown in Fig. 3. The average diameter and length of NCC from cotton were measured as 18.4 ± 7.2 nm and 297.7 ± 98.9 nm, respectively (using *Image J analysis*) (Fig. 4). The presence of carbon nanodots as one of the by-product of the reaction is evident from TEM. This could not be separated successfully from the nanocellulose. The corresponding TEM images for NFC and NCC, isolated from bleached pulp are presented in the Supporting Information, Figure S3. The average hydrodynamic size distribution of 0.2% aqueous dispersion of NFC and NCC obtained from cotton (determined through dynamic light scattering method) was found to be 1208 ± 288.8 nm and 234 ± 45.11 nm for NFC and 389.3 ± 39.2 nm for NCC. The DLS data for NFC and NCC isolated from cotton and bleached pulp is presented in Supporting Information Figure S4.

The structural characteristics of NFC and NCC were compared with those of cotton using FTIR (Supporting Information, Figure S5. The O–H stretching in cotton that appears at 3436 cm^{-1} (arising out of intramolecular H-bonds and intermolecular H-bonds in cellulose at 3335 and 3285 cm^{-1}, respectively) as well as that for adsorbed water is shifted to lower frequency of 3396 cm^{-1} in the case of NFC and NCC. Further, narrowing and deepening of this peak, suggested the presence of higher extent of intermolecular H-bonds among the cellulose molecules possibly due to the removal of the amorphous components. This is also reflected by the increasing frequency of the pyranose ring C–O stretching from 1030 cm^{-1} in the case of cotton to 1042 cm^{-1} for NFC and 1052 cm^{-1} for NCC (the increasing frequency is most likely due to lesser constraint for C–O stretching, made possible

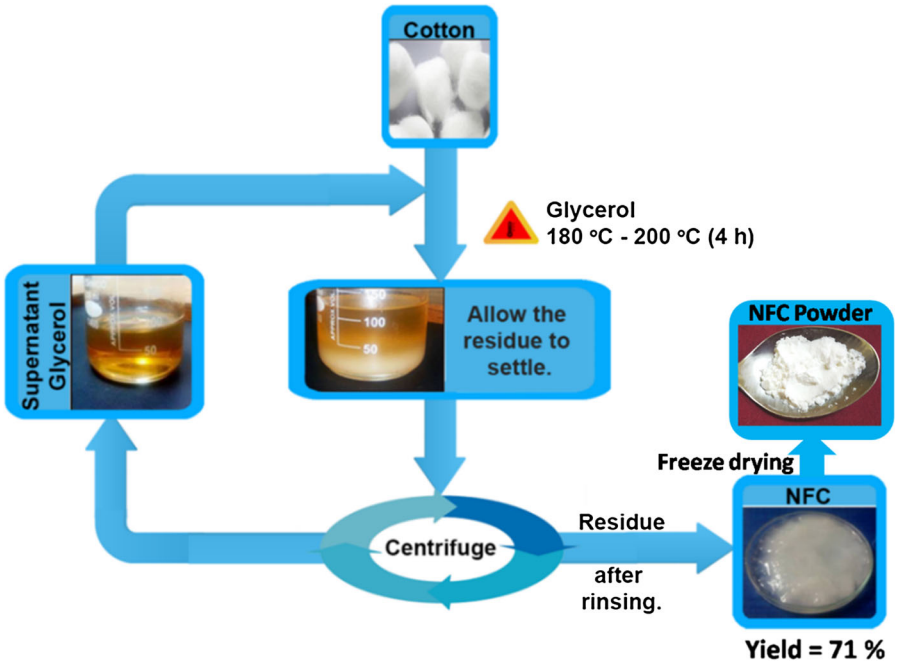

Scheme 1 Conversion of cotton into NFC through thermal treatment in glycerol

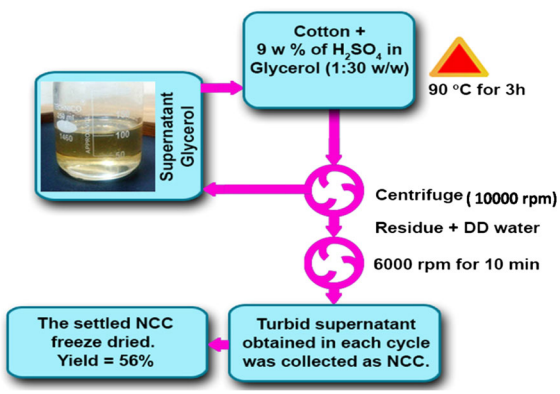

Scheme 2 Conversion of cotton into NCC by thermal treatment in 1 M solution of H_2SO_4 in glycerol

by the removal of some non-bonded interactions). The asymmetric and symmetric C–H stretching frequencies observed in surgical cotton at 2923 and 2844 cm^{-1} is shifted to 2908 cm^{-1} (asymmetric) in the case of NFC and NCC. The absence of the symmetric C–H stretching frequency in NFC and NCC suggests the removal of aliphatic component(s) arising from cotton. Further a prominent peak observed at 1726 cm^{-1} in cotton (possibly due to ester or amide groups arising from the protein or hemicellulose or lignin) is not observed in NFC and NCC suggesting their removal in the course of the treatment. The peak observed at 1615 cm^{-1} in the case of cotton might be due to lignin (C=C stretching). This disappears in the case of NFC and NCC and instead a new peak at 1640 cm^{-1} attributed to adsorbed water (O–H bending) is observed. This is also confirmed by TGA analysis of NFC and NCC that confirms the presence of volatiles that are lost from the samples in the vicinity of 100 °C. The marginal change in the signature peaks of cellulose present in the cotton such as C–H bending (asymmetric for cotton, NFC, NCC: 1457, 1440 and 1428 cm^{-1}; symmetric for cotton, NFC and NCC: 1378, 1368, and1366 cm^{-1}; as well as 1313, 1313 and 1315 cm^{-1}), C–O stretching (asymmetric & symmetric for cotton, NFC and NCC: 1253, 1237, 1240 & 1154, 1115, 1109 and 1115 cm^{-1}) and pyranose ring C–O stretching (1030, 1042 and 1052 cm^{-1}, respectively for cotton, NFC and NCC) indicate that the treatment with glycerol as well as 1 M sulphuric acid in glycerol did not alter the molecular structure of cellulose significantly but may have eliminated some of the weaker interactions that restricted the specific vibrations in cotton.

The stability of nanocellulose dispersion is critical for many applications. The zeta potential distribution for 0.2 wt% aqueous dispersion of NCC is presented

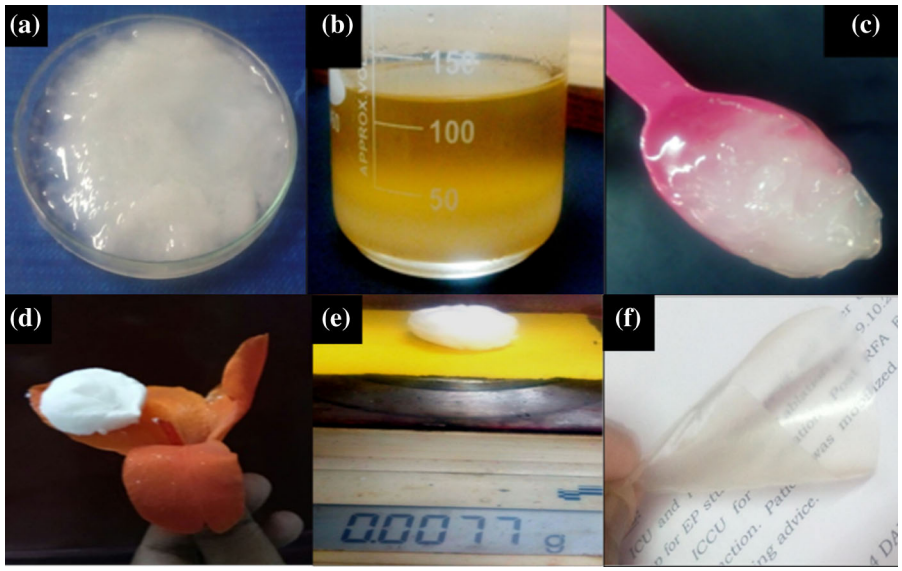

Fig. 1 Photographs of **a** NFC obtained after treatment in hot glycerol after centrifugal separation and water rinsing as shown in Scheme 1, **b** NCC that settled after heat treatment in 1 M H_2SO_4 in glycerol, **c** NCC dispersion before freeze drying, **d**, **e** NCC aerogel obtained after freeze drying, and **f** transparent flexible film of NCC

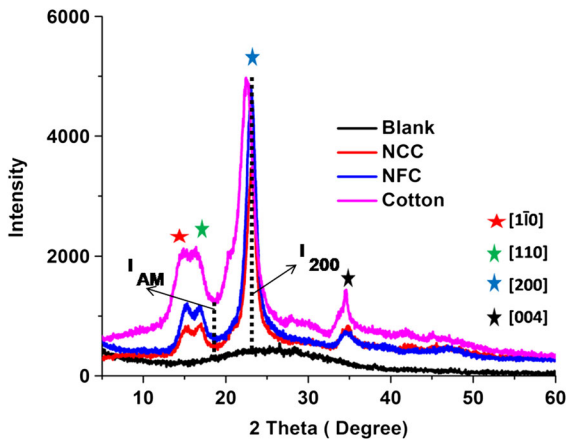

Fig. 2 PXRD patterns of **a** cotton; **b** NFC obtained from cotton through hot-glycerol treatment; **c** NCC obtained from cotton by treatment with 1 M H_2SO_4 in glycerol. The diffraction pattern in black in all the cases is from microscopic glass slide used as support (blank)

in Fig. 5a. The average value of the zeta potential for NCC derived from cotton was determined to be − 27.7 ± 3.73 mV. This indicates that there could be considerable electrostatic repulsion between the particles due to the surface charge arising probably due to the presence of carboxylic acid functional groups. This mutual repulsion can prevent aggregation between the nanocrystals and result in good dispersion stability.

The average value of the zeta potential for 0.2 wt% aqueous dispersion of NFC isolated from cotton was found to be − 9.0 ± 4.51 mV (Fig. 5b). The NFC prepared through the hot glycerol treatment has comparatively larger sized fibres than the size of NCC. Therefore they settled down within minutes. Moreover, the hot glycerol treatment could not be expected to introduce any surface functionalization on NFC, which is required to induce particle repulsion. Therefore NFC showed poor dispersion stability. The zeta potential of NCC and NFC isolated from bleached cellulose pulp is given in Supporting Information Figure S6.

The photographs of a 1% w/w aqueous dispersion of NCC (cotton) with time are presented in Fig. 6. This dispersion is found to be very stable and homogeneous up to 4 h. NCC particle aggregation began to occur after 24 h and the supernatant appeared to become more transparent after 7 days suggesting that flocculation was taking place over this time. It may be noted that longer duration of hydrolysis, higher concentration of acid as well as higher temperature of treatment could have resulted in more stable dispersion of NCC due to extensive surface functionalization.

The transparency of the NCC film prepared by evaporating 1% aqueous dispersion of NCC in glass Petridish was characterised by diffuse reflectrance

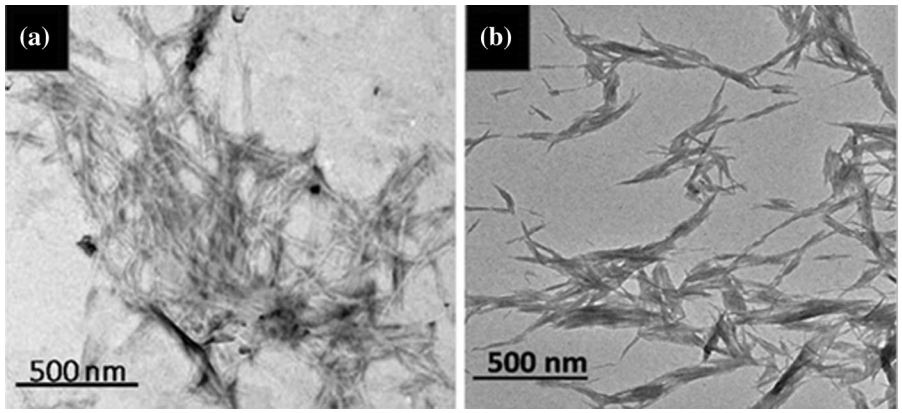

Fig. 3 TEM micrographs of **a** NFC from cotton, **b** NCC from cotton

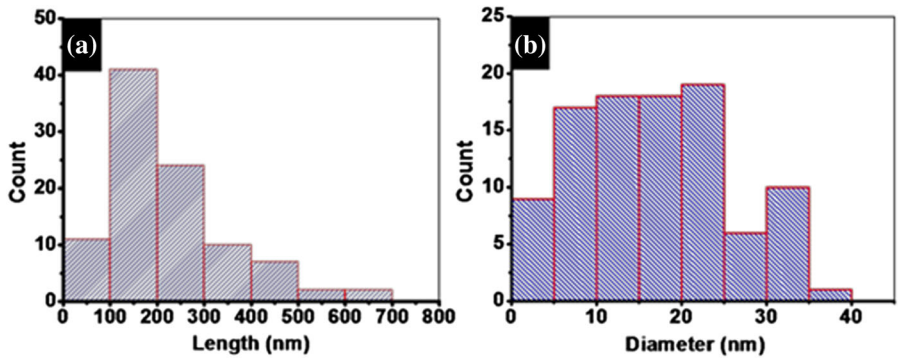

Fig. 4 Average size distributions of NCC from cotton

spectroscopy (Fig. 7). The film showed high transparency in the visible region from 400 to 800 nm with a maximum transparency of 68.9% observed around 503 nm. In the case of NFC, transparent film was not obtained by the evaporation of the NFC dispersion due to the absence of surface modification and fiber agglomaration.

Mechanism

The supernatant obtained, post hot-glycerol treatment, after NFC isolation exhibited a pH of 7 (a small quantity of double distilled and deionised water was added to make the measurement). This suggested that acids such as formic acid, which are normally formed upon high temperature treatment of cellulose, are not present in the reaction mixture under the present treatment conditions in hot glycerol (180 to 200 °C). This automatically ruled out acid-catalyzed breakdown of cellulose upon treatment in hot glycerol leading to the formation of NFC. The glycerol-supernatant tested positive to Tollen'sreagent (Supporting Information Figure S7) suggesting the presence of reducing agents. It also formed a phenylhydrazone with a melting point of 134 °C suggesting the presence of carbonyl functional groups. The formation of reducing sugar in the process was confirmed by treating the supernatant of the reaction mixture with yeast in water, which was left undisturbed for 14 days. Then the solution was distilled at 100 °C under reduced pressure. The distillate thus obtained was analysed using NMR. The ^{1}H NMR spectrum showed the presence of ethanol along with lactic acid and acetic acid (Supporting Information Figure S8). This experiment strongly supports the formation of reducing sugar in the hot glycerol treatment for the isolation of NFC. In order to test for the presence of free radicals during the treatment, a part of the glycerol-supernatant was taken out and reacted with 2,2-diphenyl-1-picrylhydrazyl (DPPH) in methanol (violet in color). An instant change in color from violet to yellow was observed. The UV-visible

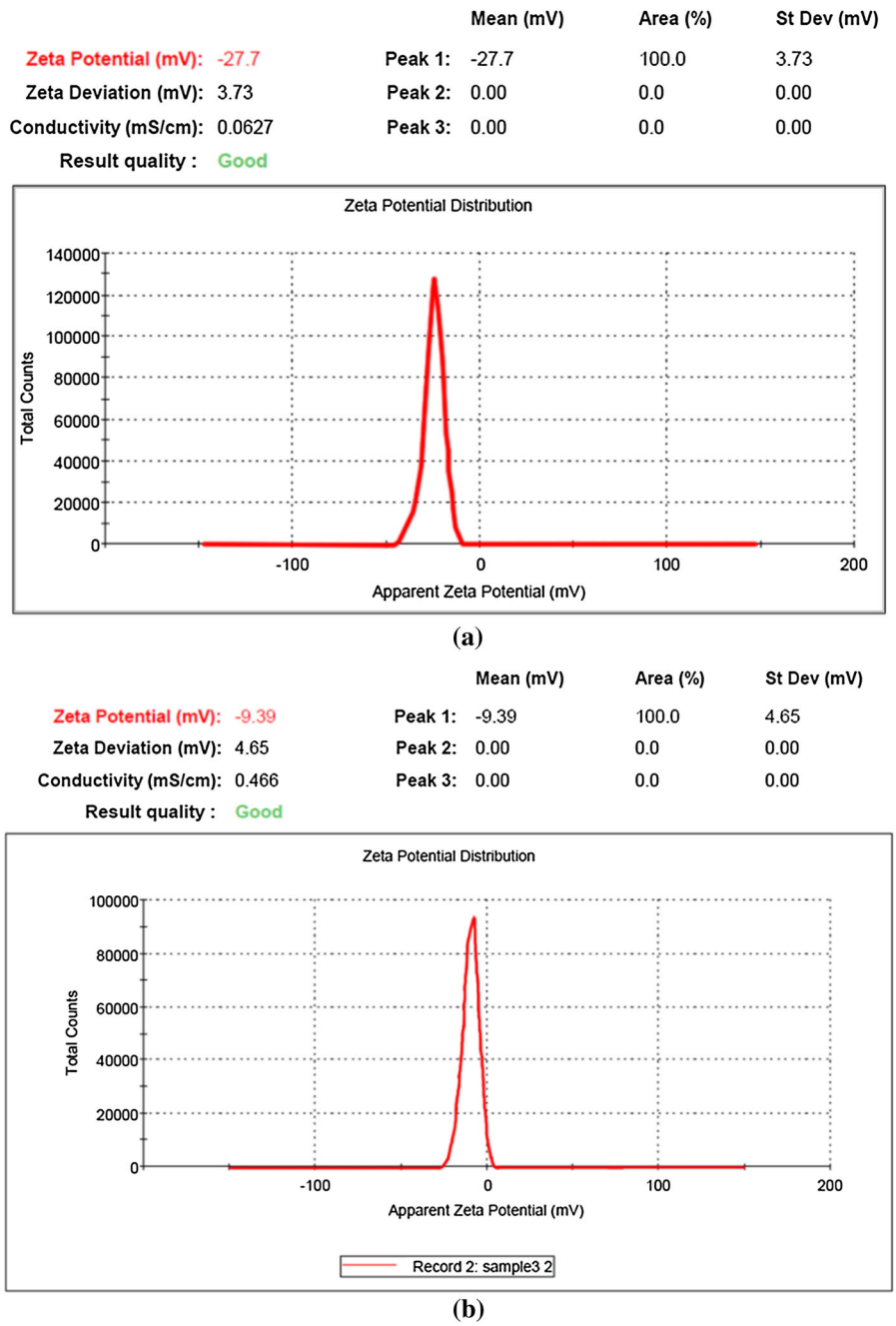

Fig. 5 Zeta potential distribution of **a** NCC and **b** NFC isolated from surgical cotton

spectral analysis (Supporting Information S9) indicated the disappearance of the peak observed at 516 nm for DPPH while similar reaction with hot-glycerol (control) showed that the maximum at 516 nm did not disappear and the color of the mixture continued to remain violet. These experiments confirmed the formation of free radicals when cotton is treated with hot glycerol alone. The formation of radicals is also consistent with the earlier results on the formation of free radicals in low temperature pyrolysis of cellulose. It was reported that the level of water evolved from cellulose heated at 180 °C in air was two times that observed in nitrogen atmosphere suggesting

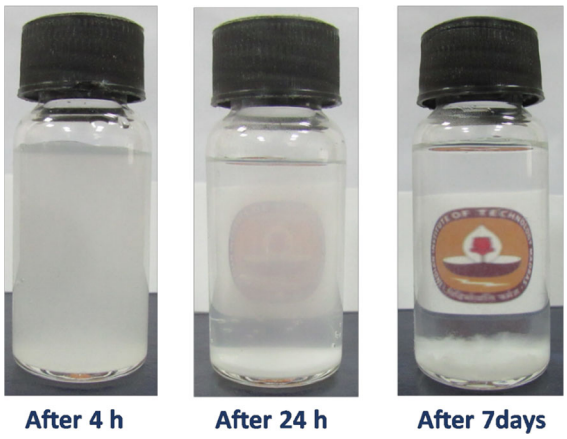

Fig. 6 Photographs showing the flocculation of NCC dispersion with time

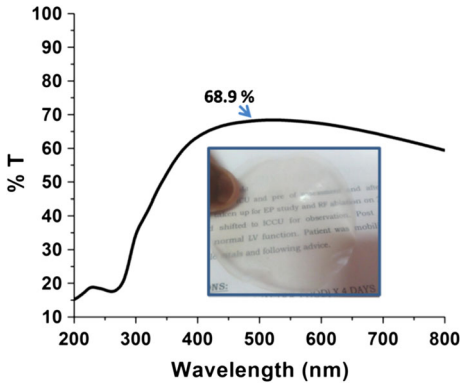

Fig. 7 Diffuse reflectance spectrum of NCC film

that there must be a free-radical route for the formation of water (Shafizadeh 1968).

In addition to the free radical mechanism of fragmentation of cellulose, it has been reported that thermal dehydration in cellulose can occur in the temperature range 150–240 °C (Navell and Zeronian 1985; Pastorova et al. 1993; Tang and Bacon 1964). In general, elimination of water from cellulose due to chemical process starts around 180 °C that is attributed to the conversion of hydroxyl groups to keto groups. This has been shown to occur in the amorphous regions of cellulose (Basch and Lewin 1973). In the experiments reported here, the fragmentation, depolymerisation, elimination, etc., reported in the literature in the absence of glycerol must be taking place in the presence of glycerol that would facilitate uniform heat transfer. It could be happening through the free radical pathway as well as the dehydration-elimination pathways as reported. Since glycerol is known to plasticize chitosan (Epure et al. 2011), we examined if it could plasticize the amorphous regions of cotton under the experimental conditions reported here. The PXRD of cellulose after the absorption of glycerol, shown in Supporting Information Figure S10, suggested the plasticization through the formation of a broad amorphous halo in the 2θ region 30 to 70. The plasticization may have facilitated uniform heat transfer and thereby thermally initiated transformations such as low temperature pyrolysis of the amorphous regions of the cellulose leading to the reduction in polymerization, formation of free radicals (especially hydroperoxide radicals), elimination of weakly bounded water, intra- and intermolecular eliminations and formation of carbonyl, carboxylic acid functional groups (Collard and Blin 2014; Lu et al. 2011; Patwardhan et al. 2009; Scheirs et al. 2001; Shafizadeh 1982; Soltes et al. 1981; Zhou et al. 2014).

The above observations combined with literature on thermal fragmentation of cellulose suggest that the same might be taking place in the presence of glycerol. This is most likely to take place in the amorphous regions due to their relative ease of accessibility and swelling in glycerol. The enhancement in the crystallinity index of cotton due to the formation of NCC has been attributed to the dissolution of the amorphous regions of cotton in the presence of strong mineral acid.

Application of NCC as mineral admixture for cement mortar and the effect on mechanical properties of the cured composite

The NCC prepared was used as a mineral admixture as such and after surface modification with TEOS (Scheme presented in Supporting Information, Figure S11). This modification that introduces Si–O–Si bonds on the surface was carried out to enable better compatibility of NCC with the inorganic cement. Upon surface modification, the hydroxyl groups present on the surface of NCC undergo condensation with TEOS to form –Si–O–Si– mono/multi-layer coating. The SEM images of NCC without surface modification and NCC following surface modification with TEOS (TNCC) are presented in Figs. 8a, b, respectively, with the latter showing the formation of spherical particles (Stober silica) on the surface of TNCC (Stöber et al. 1968).

Based on the results from the control experiments carried out with different water/cement ratios (w/c), the one with water/cement ratio (w/c) 0.45 resulted in the highest compressive strength (35.9 ± 2.1 MPa). Therefore, the optimum w/c ratio for the remaining set of experiments with various amounts of admixtures was fixed as 0.45 (the average compressive strength of mortar cubes with different w/c ratio is shown in Supporting Information Figure S12). The average compressive strength of cement mortar cubes with different loadings of NCC and TNCC as mineral admixtures as a function of curing time (w/c ratio 0.45) is presented in Fig. 9.

The addition of NCC as an admixture to the cement mortar was found to be positively contributing to the compressive strength of the mortar. The compressive strength of cement mortar is enhanced further by increasing the NCC loading from 0.5 to 1.0%. The addition of 0.5% and 1.0% of NCC to cement mortar achieved 24% and 30% of compressive strength enhancement, respectively compared to the control (28 days water cured samples). It was not surprising that NCC/TNCC with high aspect ratio and specific strength as well as homogenised distribution throughout the cement matrix contributed to enhanced compressive strength. It was observed that when the NCC loading was beyond 1.0% of the weight of cement the cement mortar was less workable (i.e. % spread < 30), in the flow table test. The workability of cement mortar mix with different loading rate of NCC and TNCC is given in Supporting Information Figure S13. The cement mortar with 0.5% and 1.0% of TNCC resulted in 39% and 44% enhancement in the compressive strength, respectively. In contrast, around 10% TEOS surface modified microcrystalline

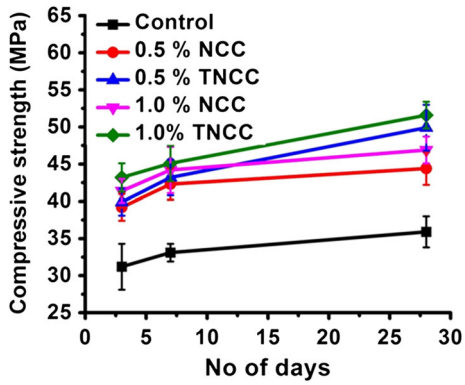

Fig. 9 Compressive strength of cement mortar cubes with varying amount of NCC and TNCC

cellulose (MCC) admixture was required to achieve the same compressive strength, which was reported in our earlier publication (Anju et al. 2016).The advantages of nano sized cellulose are its well-known higher specific strength as well as effective filling of the micro-pores within the cement mortar. With the silica-based covering on TNCC surface the better compatibility between the admixture and inorganic based cement matrix adds to the enhancement of strength.

The SEM image of 28 days water-cured cement mortar sample without the addition of any admixture is shown in Fig. 10a. The presence of large number of micro-pores within the sample is clear from this image. The SEM image of 28 days water-cured cement mortar sample with 1.0% TNCC (by dry weight of cement) is shown in Fig. 10b. From the figure, it is clear that the TNCC admixture effectively filled the pores within the mortar with adequate compatibility with cement.

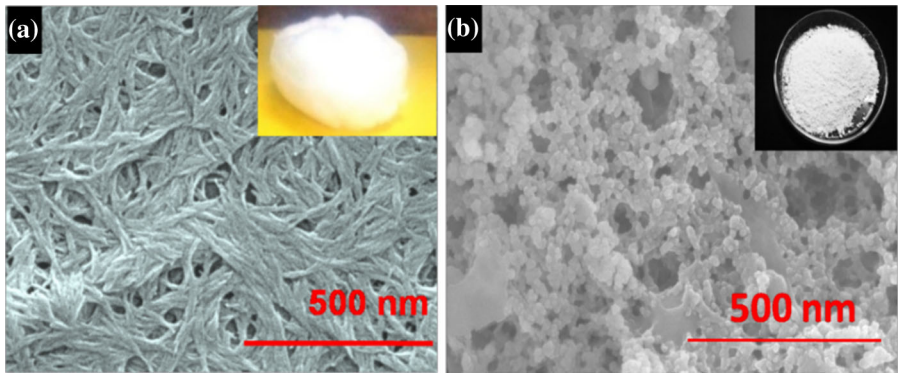

Fig. 8 SEM micrographs of **a** NCC (photograph of freeze-dried NCC in inset) and **b** TNCC (photograph of TNCC powder in inset)

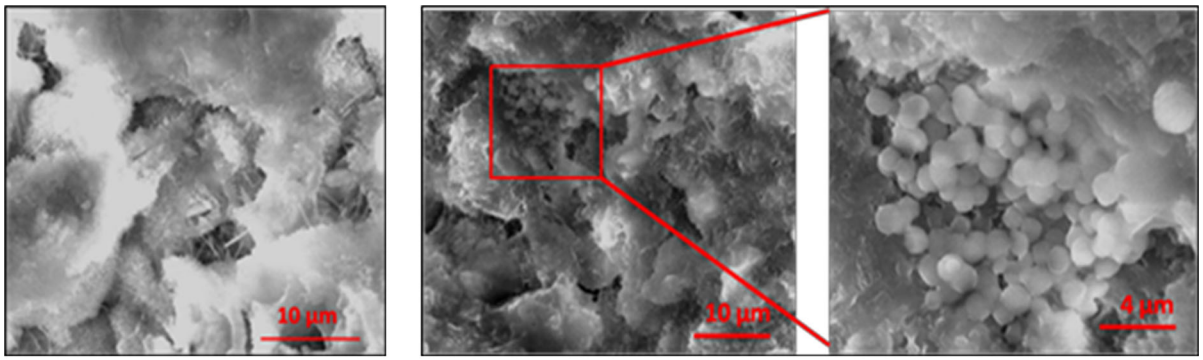

Fig. 10 SEM images of water-cured cement mortar samples: **a** control without TNCC and **b** with 1.0% TNCC by weight of cement **c** expanded image showing the compatibility of TNCC with mortar

Conclusion

A simple method of preparing nanofibrillated cellulose (NFC) from cotton is demonstrated using hot-glycerol treatment as an alternative to the energy intensive mechanical disintegration method. The 'green solvent' could be reused over several cycles. Similar heat treatment in the presence of a 1 M solution of sulphuric acid in glycerol resulted in the formation of nanocrystalline cellulose (NCC). In the process developed, we believe that glycerol function as a plasticizer of the amorphous regions enabling uniform heat transfer leading to depolymerisation/dehydration that has been reported for low as well as high temperature pyrolysis of cellulose. The depolymerisation/dehydration is catalysed by mineral acid and therefore in the presence of the mineral acid, extensive fragmentation of the amorphous regions takes place, leading to the formation of NCC. The non-use of unsustainable and harmful solvents and the absence of waste portray the eco-friendliness of the process. The low cost, industrial scalability and versatility of the process, further add to its attractiveness. We also demonstrated that NCC prepared in this manner could be utilised as an effective cement admixture. By the addition of 1% TEOS surface modified NCC, the cement mortar could achieve 51.6 ± 1.8 MPa as compressive strength, which was 44% higher than that of the blank cement mortar.

Acknowledgments The authors thank the Department of Materials and Metallurgical Engineering, IIT Madras for extending the TEM facility and Prof.S. Ramaprabhu, Department of Physics, IIT Madras for enabling zeta potential measurements and dynamic light scattering experiments. The authors thank Prof. K. Ramamurthy of the Department of Civil Engineering, IIT Madras for guiding the work on cement-reinforcement studies and testing. The work presented here is a part of Indian patent application (201841019186) filed by the authors. This work was supported by IIT Madras.

Compliance with ethical standards

Conflict of interest The authors declare no competing financial interests.

References

Abdelmouleh M, Boufi S, Ben Salah A, Belgacem MN, Gandini A (2002) Interaction of silane coupling agents with cellulose. Langmuir 18:3203–3208. https://doi.org/10.1021/la011657g

Anju TR, Ramamurthy K, Dhamodharan R (2016) Surface modified microcrystalline cellulose from cotton as a potential mineral admixture in cement mortar composite. Cem Concr Compos 74:147–153. https://doi.org/10.1016/j.cemconcomp.2016.09.003

ASTM C109 (2013) Test method for compressive strength of hydraulic cement mortar. American Society for Testing and Materials, West Conshohocken

ASTM C1437 (2013) Test method for flow of hydraulic cement mortar. American Society for Testing and Materials, West Conshohocken

Basch A, Lewin M (1973) The influence of fine structure on the pyrolysis of cellulose. I. Vacuum pyrolysis. J Polym Sci Part A Polym Chem 11:3071–3093. https://doi.org/10.1002/pol.1973.170111204

Chakraborty A (2004) Ph.D. thesis, University of Toronto

Collard FX, Blin J (2014) A review on pyrolysis of biomass constituents: mechanisms and composition of the products obtained from the conversion of cellulose, hemicelluloses and lignin. Renew Sustain Energy Rev 38:594–608. https://doi.org/10.1016/j.rser.2014.06.013

Dai D, Fan M, Collins P (2013) Fabrication of nanocelluloses from hemp fibers and their application for the reinforcement of hemp fibers. Ind Crops Prod 44:192–199. https://doi.org/10.1016/j.indcrop.2012.11.010

Dinand E, Chanzy H, Vignon RM (1999) Suspensions of cellulose microfibrils from sugar beet pulp. Food Hydrocoll 13:275–283. https://doi.org/10.1016/S0268-005X(98)00084-8

Dufresne A, Cavaille JY, Vignon MR (1997) Mechanical behavior of sheets prepared from sugar beet cellulose microfibrils. J Appl Polym Sci 64:1185–1194. https://doi.org/10.1002/(SICI)1097-4628(19970509)64:6%3c1185:AID-APP19%3e3.0.CO;2-V

Duran N, Lemes AP, Seabra AB (2012) Review of cellulose nanocrystals patents: preparation, composites and general applications. Recent Pat Nanotechnol 6:16–28. https://doi.org/10.2174/187221012798109255

Epure V, Griffon M, Pollet E, Avérous L (2011) Structure and properties of glycerol-plasticized chitosan obtained by mechanical kneading. Carbohydr Polym 83:947–952. https://doi.org/10.1016/j.carbpol.2010.09.003

Espinosa SC, Kuhnt T, Foster EJ, Weder C (2013) Isolation of thermally stable cellulose nanocrystals by phosphoric acid hydrolysis. Biomacromolecules 14:1223–1230. https://doi.org/10.1021/bm400219u

Islam MT, Alam MM, Patrucco A, Montarsolo A, Zoccola M (2014) Preparation of nanocellulose: a review. AATCC J Res 1:17–23. https://doi.org/10.14504/ajr.1.5.3

Jia X, Chen Y, Shi C, Ye Y, Wang P, Zeng X, Wu T (2013) Preparation and characterization of cellulose regenerated from phosphoric acid. J Agric Food Chem 61:12405–12414. https://doi.org/10.1021/jf4042358

Kamel S (2007) Nanotechnology and its applications in lignocellulosic composites, a mini review. Express Polym Lett 1:546–575. https://doi.org/10.3144/expresspolymlett.2007.78

Kargarzadeh H, Ioelovich M, Ahmad I, Thomas S, Dufresne A (2017) Handbook of nanocellulose and cellulose nanocomposites. Wiley-VCH Verlag GmbH & Co. KgaA, New York. https://doi.org/10.1002/9783527689972

Kaushik M, Moores A (2016) Review: nanocelluloses as versatile supports for metal nanoparticles and their applications in catalysis. Green Chem 18:622–637. https://doi.org/10.1039/C5GC02500A

Klemm D, Kramer F, Moritz S, Lindstrom T, Ankerfors M, Gray D, Dorris A (2011) Nanocelluloses: a new family of natural-based materials. Angew Chem Int Ed 50:5438–5466. https://doi.org/10.1002/anie.201001273

Kos T, Anžlovar A, Kunaver M, Huskić M, Žagar E (2014) Fast preparation of nanocrystalline cellulose by microwave-assisted hydrolysis. Cellulose 21:2579–2585. https://doi.org/10.1007/s10570-014-0315-2

Kunaver M, Anzlovar A, Zagar E (2016) The fast and effective isolation of nanocellulose from selected cellulosic feedstocks. Carbohydr Polym 148:251–258. https://doi.org/10.1016/j.carbpol.2016.04.076

Li W, Wang R, Liu S (2011) Nanocrystalline cellulose prepared from softwood kraft pulp via ultrasonic-assisted acid hydrolysis. BioResources 6:4271–4281. https://doi.org/10.15376/biores.6.4.4271-4281

Lu Q, Yang XC, Dong CQ, Zhang ZF, Zhang XM, Zhu XF (2011) Influence of pyrolysis temperature and time on the cellulose fast pyrolysis products: analytical Py-GC/MS study. J Anal Appl Pyrol 92:430–438. https://doi.org/10.1016/j.jaap.2011.08.006

Lu QL, Li XY, Tang LR, Lu BL, Huang B (2015) One-pot tandem reactions for the preparation of esterified cellulose nanocrystals with 4-dimethylaminopyridine as a catalyst. RSC Adv 5:56198–56204. https://doi.org/10.1039/C5RA08690F

Maiti S, Jayaramudu J, Das K, Reddy SM, Sadiku R, Ray SS, Liu D (2013) Preparation and characterization of nanocellulose with new shape from different precursor. Carbohydr Polym 98:562–567. https://doi.org/10.1016/j.carbpol.2013.06.029

McCann MC, Wells B, Roberts K (1990) Direct visualization of cross-links in the primary plant cell wall. J Cell Sci 96:323–334

Navell TP, Zeronian SH (1985) Intercrystalline swelling of cellulose. In: Zeronian SH, Nevell TP (eds) Cellulose chemistry and its applications. Wiley, New York. https://doi.org/10.1002/pol.1987.140250212

Pääkko M, Ankerfors M, Kosonen H, Nykänen A, Ahola S, Österberg M, Ruokolainen J, Laine J, Larsson PT, Ikkala O (2007) Enzymatic hydrolysis combined with mechanical shearing and high-pressure homogenization for nanoscale cellulose fibrils and strong gels. Biomacromolecules 8:1934–1941. https://doi.org/10.1021/bm061215p

Park S, Baker JO, Himmel ME, Parilla PA, Johnson DK (2010) Cellulose crystallinity index: measurement techniques and their impact on interpreting cellulase performance. Biotechnol Biofuels 3:10

Pastorova I, Arisz PW, Boon JJ (1993) Preservation of D-glucose-oligosaccharides in cellulose chars. Carbohydr Res 248:151–165. https://doi.org/10.1016/0008-6215(93)84123-N

Patwardhan PR, Satrio JA, Brown RC, Shanks BH (2009) Product distribution from fast pyrolysis of glucose-based carbohydrates. J Anal Appl Pyrol 86:323–330. https://doi.org/10.1016/j.jaap.2009.08.007

Rajinipriya M, Nagalakshmaiah M, Robert M, Elkoun S (2018) Importance of agricultural and industrial waste in the field of nanocellulose and recent industrial developments of wood based nanocellulose: a review. ACS Sustain Chem Eng 6:2807–2828. https://doi.org/10.1021/acssuschemeng.7b03437

Sadeghifar H, Filpponen E, Clarke SP, Brougham DF, Argyropoulos DS (2011) Production of cellulose nanocrystals using hydrobromic acid and click reactions on their surface. J Mater Sci 46:7344–7355. https://doi.org/10.1007/s10853-011-5696-0

Saito T, Kimura S, Nishiyama Y, Isogai A (2007) Cellulose nanofibers prepared by TEMPO-mediated oxidation of native cellulose. Biomacromolecules 8:2485–2491. https://doi.org/10.1021/bm0703970

Sannino A, Demitri C, Madahiele M (2009) Biodegradable cellulose-based hydrogels: design and applications. Materials 2:353–373. https://doi.org/10.3390/ma2020353

Scheirs J, Camino G, Tumiatti W (2001) Overview of water evolution during the thermal degradation of cellulose. Eur

Polym J 37:933–942. https://doi.org/10.1016/S0014-3057(00)00211-1

Segal L, Creely JJ, Martin AE, Conrad CM (1959) An empirical method for estimating the degree of crystallinity of native cellulose using the X-ray diffractometer. Text Res J 29:786–794. https://doi.org/10.1177/004051755902901003

Serizawa T, Sawada T, Okura H, Wada M (2013) Hydrolytic activities of crystalline cellulose nanofibers. Biomacromolecules 14:613–617. https://doi.org/10.1021/bm4000822

Shafizadeh F (1968) Pyrolysis and combustion of cellulosic materials. Adv Carbohydr Chem 23:419–474. https://doi.org/10.1016/S0096-5332(08)60173-3

Shafizadeh F (1982) Introduction to pyrolysis of biomass. J Anal Appl Pyrol 3:283–305. https://doi.org/10.1016/0165-2370(82)80017-X

Soltes EJ, Wiley AT, Lin SCK (1981) Biomass pyrolysis-towards an understanding of its versatility and potentials. Biotechnol Bioeng Symp Ser 11:125–136

Stöber W, Fink A, Bohn E (1968) Controlled growth of monodisperse silica spheres in the micron size range. J Colloid Interface Sci 26:62–69. https://doi.org/10.1016/0021-9797(68)90272-5

Tang MM, Bacon R (1964) Carbonization of cellulose fibers—I. Low temperature pyrolysis. Carbon 2:211–220. https://doi.org/10.1016/0008-6223(64)90035-1

Vom Stein T, Grande P, Sibilla F, Commandeur U, Fischer R, Leitner W, Domínguez de María P (2010) Salt-assisted organic-acid-catalysed depolymerization of cellulose. Green Chem 12:1844–1849. https://doi.org/10.1039/C0GC00262C

Xiao YT, Chin WL, Abd Hamid SB (2015) Facile preparation of highly crystalline nanocellulose by using ionic liquid. Adv Mater Res 1087:106–110. https://doi.org/10.4028/www.scientific.net/AMR.1087.106

Yu H, Qin Z, Liang B, Liu N, Zhou Z, Chen L (2013) Facile extraction of thermally stable cellulose nanocrystals with a high yield of 93% through hydrochloric acid hydrolysis under hydrothermal conditions. J Mater Chem A 1:3938–3944. https://doi.org/10.1039/C3TA01150J

Zhou X, Nolte MW, Mayes HB, Shanks BH, Broadbelt LJ (2014) Experimental and mechanistic modeling of fast pyrolysis of neat glucose-based carbohydrates. 1. Experiments and development of a detailed mechanistic model. Ind Eng Chem Res 53:13274–13289. https://doi.org/10.1021/ie502259w

Zimmermann T, Bordeanu N, Strub E (2010) Properties of nanofibrillated cellulose from different raw materials and its reinforcement potential. Carbohydr Polym 79:1086–1093

Publisher's Note Springer Nature remains neutral with regard to jurisdictional claims in published maps and institutional affiliations.